CSIRO PUBLISHING

www.publish.csiro.au/journals/ijwf *International Journal of Wildland Fire*, 2003, **12**, 167–174

Calculation of fire spread rates across random landscapes*

Mark A. Finney

USDA Forest Service, Fire Sciences Laboratory, Rocky Mountain Research Station, PO Box 8089, Missoula, MT 59807, USA. Telephone: +1 406 329 4832; email: mfinney@fs.fed.us

Abstract. An approach is presented for approximating the expected spread rate of fires that burn across 2-dimensional landscapes with random fuel patterns. The method calculates a harmonic mean spread rate across a small 2-dimensional grid that allows the fire to move forward and laterally. Within this sample grid, all possible spatial fuel arrangements are enumerated and the spread rate of an elliptical fire moving through the cells is found by searching for the minimum travel time. More columns in the sample grid are required for accurately calculating expected spread rates where very slow-burning fuels are present, because the fire must be allowed to move farther laterally around slow patches. This calculation can be used to estimate fire spread rates across spatial fuel mixtures provided that the fire shape was determined from wind and slope. Results suggest that fire spread rates on random landscapes should increase with fire size and that random locations of fuel treatments would be inefficient in changing overall fire growth rates.

Introduction

Large wildland fires frequently burn in environments that are spatially variable, but models and methods for predicting fire spread rates have been developed mainly for conditions that are spatially uniform (Rothermel 1972, 1983; Andrews 1986; Catchpole *et al.* 1998). Fire growth simulations (e.g. Finney 1998; Richards 2000) can accommodate many kinds and scales of spatial and temporal heterogeneity and generate detailed maps of fire behavior. Simulations, however, require explicit data for describing spatial and temporal conditions and thus pertain narrowly to the particular circumstances of that environmental scenario. For a broad range of practical applications, like operational fire predictions (Rothermel 1991; Wiitala and Carlton 1994) and fire and fuels planning (USDA Forest Service 1987; Fried *et al.* 1988; Anderson *et al.* 1998; Schaaf *et al.* 1998), a more general approach for characterizing fire spread in heterogeneous conditions is needed. A general model may also provide theoretical insight into fire behavior at fine and coarse spatial scales.

Several calculations exist for predicting fire spread rates in mixed fuel types. All are dependent on assumptions of spatial scale and pattern compared with fire size. If fuels vary at coarse scales relative to the fire and the number of discrete fuel types are few, fire behavior in each type can be calculated and considered separately (Rothermel 1983, 1991). If fire can be assumed to spread within each fuel type τ proportional to its frequency p_τ (i.e. no spread between fuel types), the expected spread rate will be the area-weighted average of spread rates r_τ among n_τ types (Rothermel 1983; Brown 1981, 1982; Fujioka 1985; Salazar 1985):

$$E[r_0] = \sum_{\tau=1}^{n_\tau} p_\tau r_\tau. \quad (1)$$

The expected spread rate for fire spreading in one direction through strips of homogeneous fuel normal to their orientation at a rate independent of adjacent fuel types is the harmonic mean (Fujioka 1985; Martin 1988; Catchpole *et al.* 1989):

$$E[r_1] = \left(\sum_{\tau=1}^{n_\tau} \frac{p_\tau}{r_\tau} \right)^{-1}. \quad (2)$$

A variant of this fuel geometry, where the spread rate in each fuel type depends on the fuel type immediately preceding it, was considered by Catchpole *et al.* (1989) as a Markov process.

These calculations do not apply to the spread rate of a fire allowed to grow in two dimensions. Under uniform and constant conditions, the spread rate of 2-dimensional fires varies as an ellipse relative to the forward direction (Van Wagner 1969; Catchpole *et al.* 1982; Richards 1990). In spatially heterogeneous conditions, however, the gross fire spread rate and shape depend on the relative properties of the fuels and their specific topological arrangements because a fire can burn laterally around obstacles.

10.1071/WF03010 1049-8001/03/020167

This paper develops a method for estimating the expected fire spread rate across a 2-dimensional landscape. The idea was to resolve the details of 2-dimensional fire growth within the simplified domain of a small sample area and then combine them statistically to infer properties about the average behavior among samples and across the whole landscape. Purely random spatial arrangements on a regular square lattice were used for developing the methods and were not intended to apply to specific actual vegetation or fuel types.

Methods

The approach developed here applies to a landscape of uniform topography having a 2-dimensional random mixture of n_τ fuel types, each occurring with a constant frequency p_τ and having a characteristic spread rate r_τ in a common direction (i.e. constant weather). A fire burning across this landscape would be observed to make direct progress through the faster fuel patches by heading, and sometimes, indirect progress around slower patches by flanking. The gross forward spread rate that this fire would achieve over a long period of time and distance could be viewed as an average of these periods of fast and slow spread. Similarly, the distances burned during these time periods could be considered as a series of strips running perpendicular to the forward spread direction. Described in terms of distance, this fuel-strip geometry is consistent with the assumptions of the harmonic mean (equation 2), and suggests a way to calculate the average fire spread rate if the 2-dimensional variation in fire spread and fuels could be characterized within the strips.

To evaluate the use of the harmonic mean for this scenario, two methods were used to define the relevant 2-dimensional strip:

(1) Using an area of fixed length and width (n_{cols} by n_{rows}); and
(2) Using an area with a variable width.

In both cases, the random fuel bed was approximated as a regular lattice of square cells, referred to as a 'sample grid' because it represents a small sample from the landscape. The variable grid permits lateral detours around fuels in the fixed grid. A square lattice is adequate to represent fuel patterns that can be approximated by regular decomposition into square cells but will introduce error for patterns of curving geometry that cannot be accurately approximated this way.

The expected spread rate in one direction across a 2-dimensional area involves a formula similar to the harmonic mean:

$$E[r_2] = \left(\sum_{i=1}^{N} \frac{p_i}{r_i} \right)^{-1} . \qquad (3)$$

For a sample grid of fixed size (Fig. 1*a*), N is the number of possible fuel configurations within the grid ($N = n_\tau^{n_{\text{rows}} n_{\text{cols}}}$); p_i is the probability of the ith fuel configuration within the sample grid (i.e. product of all p_τ); and r_i is the spread rate associated with it. The spread rate r_i is the fastest spread rate through the fuel configuration in the grid (i.e. through the route allowing fire to reach the other side the soonest). Equation (3) also applies to the variable grid (Fig. 1*b*) when the N fuel permutations are increased ($N = n_\tau^{n_{\text{rows}}(n_{\text{cols}}+2j)} n_\tau^{2j}$) to account for j extra columns on each side of the fixed grid and cells in an extra partial row that allows flanking around the original grid. Calculations with the variable grid will be distinguished as $\mathrm{E}[r_{2,j}]$.

Spread rates through the sample grids

To estimate r_i for each of N fuel configurations, a fixed sample grid (Fig. 1*a*) or variable sample grid (Fig. 1*b*) was populated with the spread rates associated with the fuel types in that configuration. The fire spread rate r_i for a particular fuel configuration was then obtained by searching for the minimum travel time of an elliptical fire shape moving from the bottom to the top of the sample grid (Finney 2002). This minimum-time algorithm was similar to the shortest path methods from graph theory (Moser 1991; Cheng and House 1996). It is appropriate if the size of the fuel patches is large enough that fire behavior can be assumed independent of neighboring types except for geometric effects on fire orientation (unlike models by Frandsen and Andrews 1979; Catchpole *et al.* 1989; Taplin 1993). The methods compute the travel time across cells using equations for elliptical expansion (Catchpole *et al.* 1982) along straight line transects among nodes (interior cell corners) of the sample grid (Finney 2002). Each node is an independent point-source fire ignition, consistent with Huygens' principle (Anderson *et al.* 1982), and each transect is composed of homogeneous segments delineated by intersections with cell boundaries and/or nodes. An ellipse is the most common and simplest fire shape used to describe fire growth under uniform and constant conditions (Van Wagner 1968; Alexander 1985; Richards 1990). The eccentricity of the ellipse is determined primarily by wind speed (Anderson 1983; Alexander 1985). In this analysis the fire shape was assumed to be the same for all fuel types but could be specified as a fuel-dependent property.

The ignition configuration, or boundary condition, chosen to approximate the ignition interface for the average sample grid, was a series of points located at the center edge of each cell along the bottom row (Fig. 1*c*). The boundary conditions were based on observations of fire simulations using FARSITE (Finney 1998) on random fuels (see below) that showed that the fire front approaching any cell within a large landscape was an elliptical curve with a size and juxtaposition determined by the upwind fuel patterns. Mixed fuels generally cause the fire to split into narrow fingers that then expand laterally when encountering patches of slower-burning fuels. For the fixed grid, each cell along the windward row was ignited because the fire was assumed larger than the scale of fuel heterogeneity. For the variable grid, the extra columns did

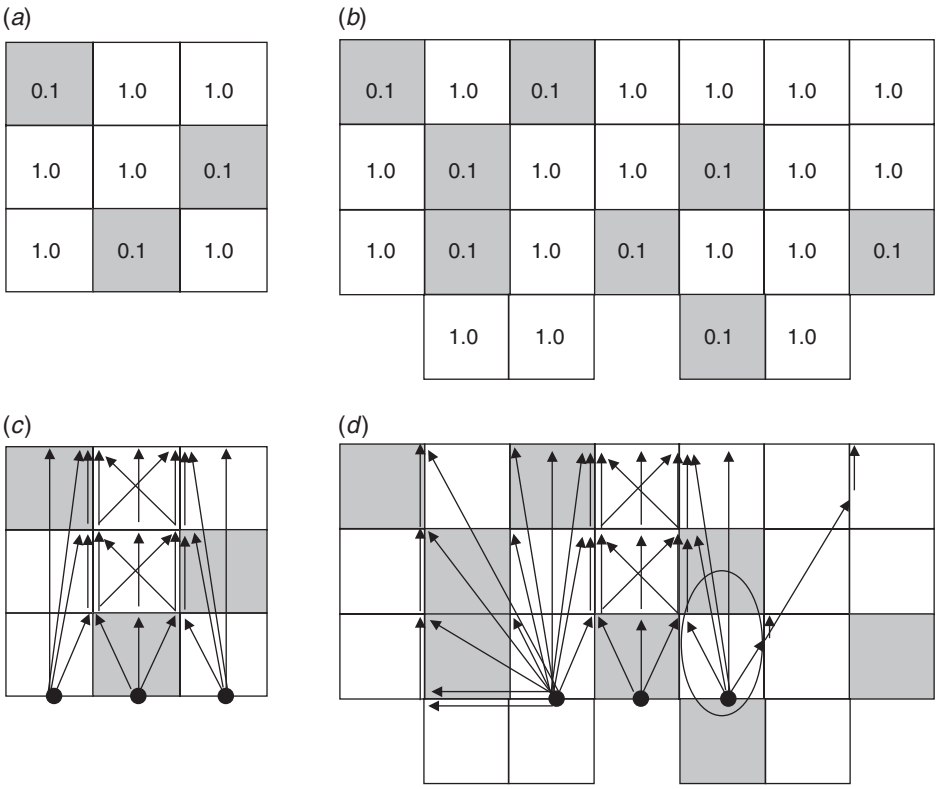

Fig. 1. Example arrangements of two fuel types: (*a*) within a sample grid with a fixed number of rows and columns (3 × 3); and (*b*) within a sample grid with two extra columns and one additional row that permits flanking around the original grid. The shaded fuel type has a relative spread rate of 0.1. These arrangements determine the spatial variability in spread rates and the probabilities of the particular fuel arrangement occurring. The minimum travel time of an elliptical fire shape to move from the ignition points (on the edge cells in the bottom row) up through the sample grid is found by searching travel routes between nodes (interior cell corners). Example routes are illustrated for (*c*) the fixed grid that has a subset of routes from (*d*) the variable-sized grid. The variable grid must also include routes at the angle of maximum flanking spread rate (indicated by the arrow through the widest part of the ellipse at right).

not receive ignition points, being ignited only by fire flanking from the edges of the original grid (Fig. 1*d*). This approximates the spatial conditions that occur when narrower fingers of fire expand laterally around obstacles. Despite numerous alternative boundary conditions, these were thought reasonable approximations to the geometry of the fire front as it approaches a sample grid in the average situation, accounting in a general way for the uncertainty in size and juxtaposition of the front as it contacts a local group of cells.

The set of routes evaluated for finding the minimum travel time is asserted to always contain the fastest possible route, given the assumed ignition configuration where all columns in the fixed grid are ignited, the grid is a square lattice, and the elliptical fire has its major axis parallel to the ordinate in all fuel types. Routes concerning the angle of maximum flanking rate were added to evaluations of the variable grid because the extra columns did not receive ignitions (Fig. 1*d*). Each fuel configuration in the sample grids has a well-defined maximum spread rate (minimum travel time), although it is not necessarily easily distinguished from all possible spread rates.

Fire growth simulations

Fire growth simulations were used to generate data for comparison with the results of the calculations. The simulations were all performed using FARSITE (Finney 1998), which expands 2-dimensional fire perimeters from vertices of a polygon using elliptical wavelets (Richards 1990, 1995). The simulations were conducted under conditions consistent with the assumptions of this analysis and included flat terrain, constant winds and fuel moistures, uniform fire shapes in each fuel type, and no acceleration or lag in fire moving from one fuel type to another. Landscape data were generated for random mixtures of two, three, and four fuel types in various proportions and replicated twice because of expected variation due to randomness of the fuel arrangements on the simulation landscapes. The random landscapes were constructed as a regular lattice of square cells, each cell having an independent random assignment of fuel type. The simulated fires were allowed to grow large (10^2 to 10^3 cells in the heading direction) compared with the cell resolution to allow

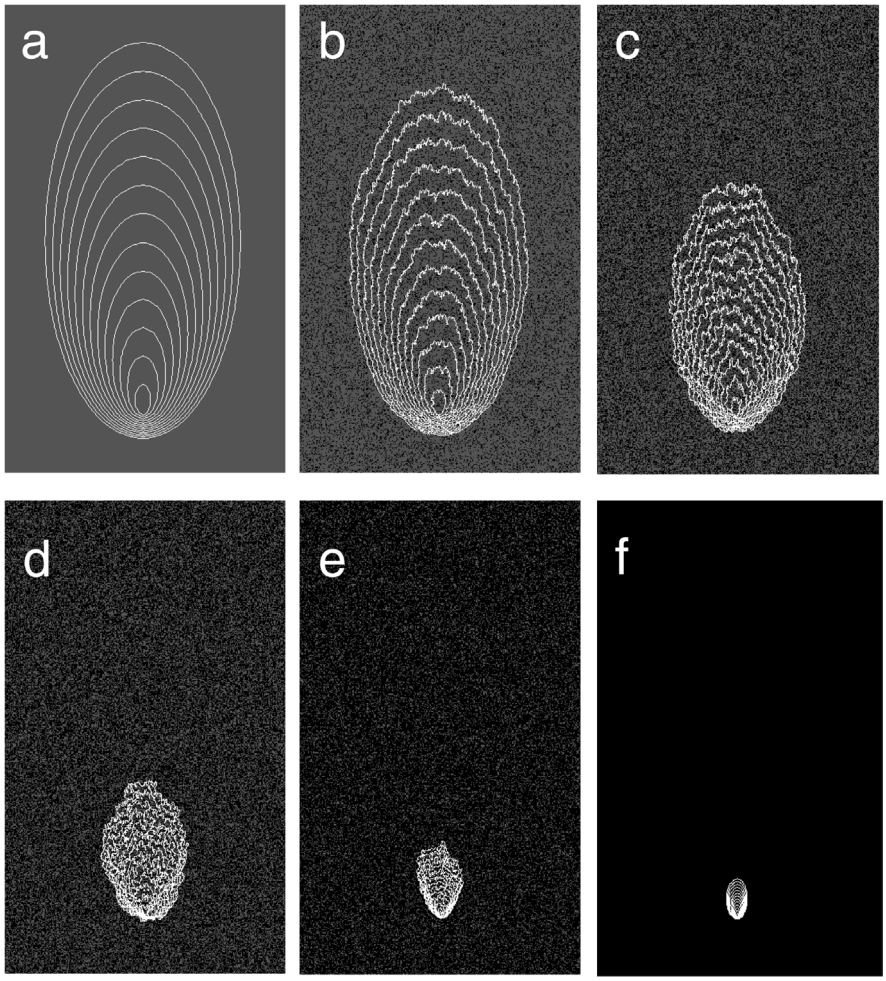

Fig. 2. Example FARSITE fire growth simulations among varying proportions of fuel two fuel types for a constant time period: (*a*) 0% slower fuel type; (*b*) 20%; (*c*) 40%; (*d*) 60%; (*e*) 80%; (*f*) 100%. The maximum forward progress of each fire was used to estimate the average spread rate that was compared with the calculated spread rates (equations 1, 2, 3) (fire length-to-breadth ratio = 2.0, slowest/fastest spread rates $SRR = 0.1$).

averaging of random effects of local fuel arrangements on fire growth over long time periods and distances. The maximum forward distance traveled by the fire at the end of a fixed time was used to calculate the average spread rate for each simulation (Fig. 2). All simulations were started from a point source. The fires quickly became larger than the resolution of the fuel cells, essentially eliminating the effects of the ignition size on the final results. An early set of simulations tested the effect of fire orientation relative to the grid axes because of the assumptions about elliptical expansion. Since the simulations produced nearly identical average spread rates for all angles, further simulations were conducted only with the fire oriented along the north–south axis.

Results

A program was written to calculate the expected spread rate using the static and variable grids in equation (3). The spread rate r_i for each fuel configuration was found by directly evaluating travel times through all routes in fixed sample grids from 1×1 to 4×4 cells. The large number of additional fuel configurations for the variable grids, however, prompted the use of a recursive method to increase efficiency. This algorithm searched for faster travel times through an increasing number of columns in the grid until none were possible or the specified limit on numbers of columns was reached. The program EXRATE was multithreaded to parallelise these calculations running on multiprocessor workstations. With 500 MHz Pentium III processors, the calculation of $\mathrm{E}[r_2]$ with two fuels using a fixed 3×3 sample grid took about 0.25 CPU-seconds. The same calculation for $\mathrm{E}[r_{2,1}]$ took about 75 CPU-seconds and 6.75-CPU hours for $\mathrm{E}[r_{2,2}]$. Some partial runs suggested that $\mathrm{E}[r_{2,3}]$ might take 100 CPU-days to calculate.

For mixtures of two fuels, the expected spread rate $\mathrm{E}[r_2]$ was found to decrease as a sigmoid curve as the proportion of slowest fuels increased (Fig. 3). This curve was in close

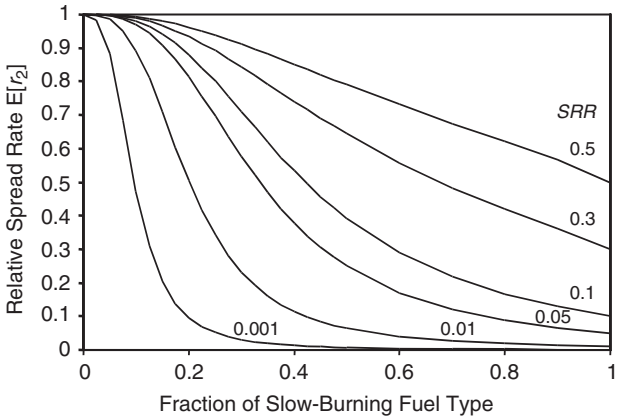

Fig. 3. Calculations of E[r_2] (equation 3) for different spread rate ratios (SRR = 0.001–0.5) showed a sigmoid trend over the range of proportions of two fuel types (fire length-to-breadth ratio = 2.0, 3 × 3 sample grid).

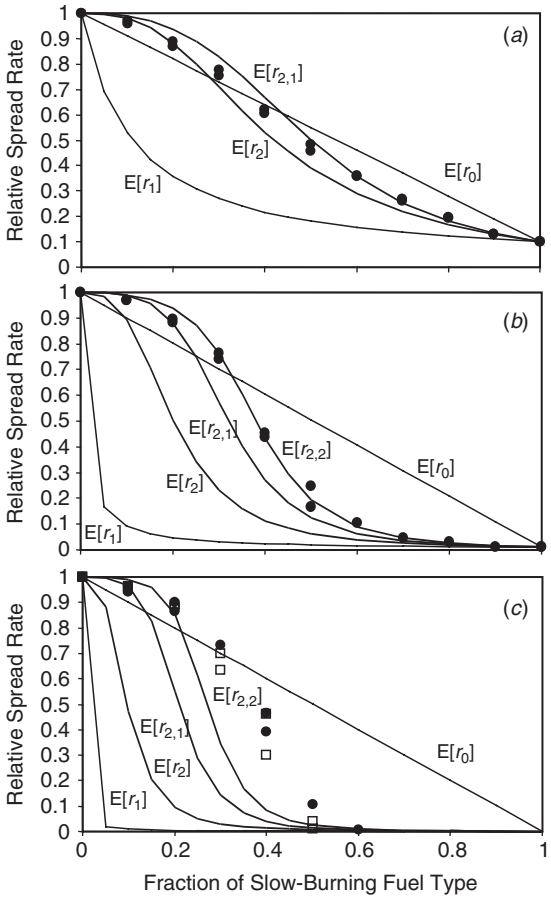

Fig. 4. Comparison of simulation data (points) for mixtures of two fuel types with expected spread rates E[r_0], E[r_1], E[r_2], and E[$r_{2,j}$] for spread rate ratios (slowest/fastest spread rates, *SRR*) of (*a*) 0.1; (*b*) 0.01; and (*c*) 0.001. Increasing width of the sample grid for E[$r_{2,j}$] was required to fit the data as the *SRR* decreased. The simulation data in (*c*) are also shown for *SRR* = 0.0 (□).

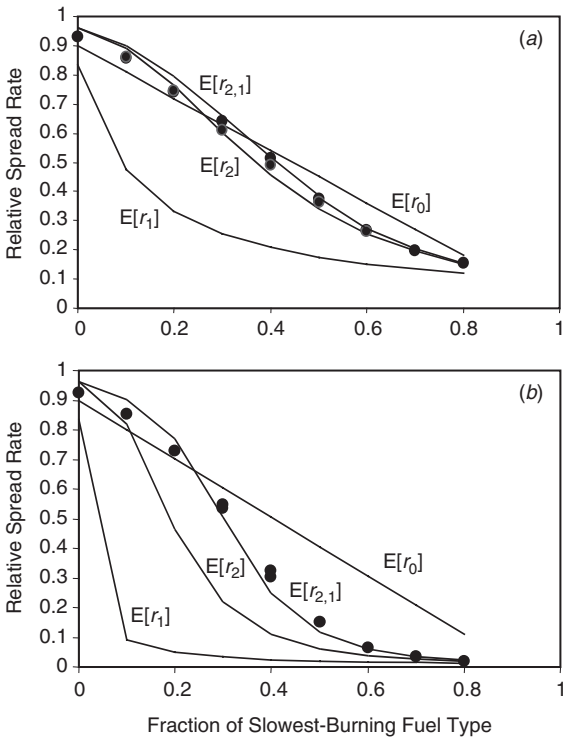

Fig. 5. The expected spread rates compared with simulation data (points) for mixtures of three fuels. The fractions of only the slowest- and fastest-burning fuel types were allowed to vary, holding the fraction of the third type constant at 0.2. Relative spread rates were fixed (*a*) at 1.0, 0.5 and 0.1, and (*b*) 1.0, 0.5, and 0.01. *LB* = 2.0, 3 × 3 sample grid.

agreement with the average spread rates measured from FARSITE simulations using a 3 × 3 fixed sample grid when relative spread rates of the slowest fuel type around 1/10th (spread rate ratio *SRR* = 0.1) (Fig. 4). As the *SRR* decreased, however, only the variable grid with additional columns produced good agreement with the simulation data. These same relationships between grid size and *SRR* were found in mixtures of three and four fuel types (Figs 5 and 6).

The expected spread rate E[r_2] increased when larger square sample grids were used (Fig. 7), reflecting the greater number of indirect routes through the grid. The expected spread rate through the 1 × 1 cell grid was the same as E[r_1], the harmonic mean (Fujioka 1985; Catchpole 1989). For comparison, the proportional mean E[r_0] was plotted, but with no contagion possible, it is a zero-dimensional calculation that is realistic only as an average for multiple fires each smaller than the scale of fuel heterogeneity.

Wider sample grids (fixed size) produced faster spread rates for all fractions of two fuels, resulting in trends in E[r_2] similar to larger grids shown in Fig. 7. Because ignitions were placed along the entire edge of the sample grid, this is interpreted as an effect of increasing the sample size on the landscape produced when the fire size becomes increasingly larger than the scale of the fuel patches. In effect, wider fires

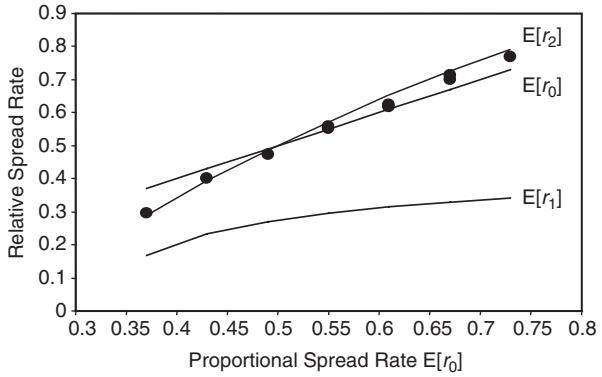

Fig. 6. The expected spread rates compared with simulation data (points) for mixtures of four fuels. Proportions were held constant at 0.2, 0.2, 0.3, and 0.3. The spread rates of two types with the smallest fractions were fixed (1 and 0.1) while the spread rates of the other two types were varied from 0.2 and 0.5 to 0.6 and 0.9. ($LB = 2.0$, 3×3 sample grid.)

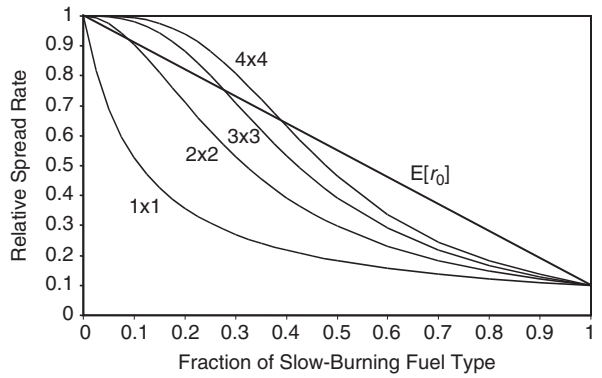

Fig. 7. The expected spread rate E[r_2] increases with the size of a square grid because wider fires have a larger sample size of the landscape in which to find faster routes. Note that E[r_2] = E[r_1] when the grid size is a single cell. ($LB = 2.0$, two fuels, slowest/fastest spread rates = 0.1.)

have greater chances of finding a faster way across a random landscape. The opposite effect occurred when the depth of the sample grid was increased. Slower E[r_2] with deeper grids results because the fire spread is restricted to the confined corridor. (As the depth of the sample grid increases for the $1 \times n$ sample grid, E[r_2] asymptotically approaches E[r_1] (or E[r_2] with a 1×1 grid). This is consistent with the assumption that the harmonic mean is the expected spread rate when fire can spread only in one dimension, completely excluding all indirect advancement of the fire through flanking.

Fire shape had a moderate effect on the expected spread rate. Length-to-breadth ratios from 1 to 8 produced a maximum difference of roughly 25% of the maximum spread rate (Fig. 8).

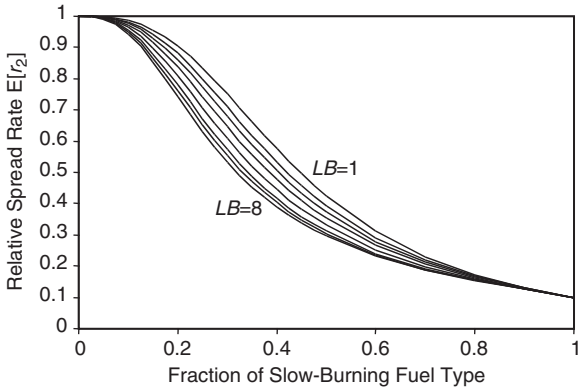

Fig. 8. The expected spread rate E[r_2] decreases with increasing eccentricity of the fire shape because of the proportion of flanking spread is smaller (3×3 sample grid, two fuels, slowest/fastest spread rates = 0.1).

Discussion

This work suggested that the harmonic mean (equation 2) could be adapted for 2-dimensional heterogeneous landscapes (equation 3) and provide good approximations to the gross fire spread rates simulated by FARSITE over a range of fuel proportions, fuel properties, and numbers of fuel types. The degree of agreement with the simulations over the range of fuel proportions, however, depended on having wider sample grids when the spread rate of the slowest-burning fuels decreased. This occurs because wider detours can produce shorter arrival times than direct routes through the slowest fuel types. In fact, grids needed to approximate the simulated spread rates when the *SRR* was less than about 0.01 were too wide to be computationally practicable. The harmonic mean applies only when all fuel types have spread rates greater than zero, meaning a different approach is required in the presence of unburnable landscape components. Fuel types commonly used in wildland fire management (Brown 1981, 1982; Anderson 1982; Salazar 1985; Forestry Canada Fire Danger Group 1992), however, have ranges in spread rate separated by less than two orders of magnitude under a wide range of environmental conditions. Since the mean spread rate E[r_2] depends on the relative spread rates of the component fuel types, it must be recalculated if the spread rates or the proportions of fuels in the mixture are changed.

Although E[r_2] generally agreed with the simulation data, some small differences were consistently observed, such as slightly over-predicted spread rates where slow fuels were rare (Fig. 4). One explanation involves the assumption that fire spreads instantly across corners of diagonal cells, but this is not actually the case in the FARSITE simulation. The simulation controls only the density of vertices on the fire front (not their location) and permits fire to be delayed when vertices fall into slower-burning fuels on both sides of a diagonal corner. A second factor may result from the use of relatively small sample grids (~3–5 cells on each side). More work would be needed to determine if a better fit to simulation data could be obtained using sample grids with different sizes and shapes (e.g. 7×5 grids) rather than the 3×3 grid used here.

Finally, it is possible that the ignition configuration of the sample grid contributed some bias to the spread rate calculations, assuming a series of point ignitions along the bottom edge of the sample grid whereas the minimum travel time algorithm solved for the first exit of the fire at the top edge. Improvements might involve a more neutral ignition configuration or variable ignitions depending on the geometry of the fire front exiting each fuel arrangement as Catchpole *et al.* (1989) did for fire acceleration.

The behavior of $E[r_2]$ with larger and wider fixed-size sample grids (Fig. 7) may suggest that broad fire fronts would be expected to spread faster than narrow ones. This follows from the assumed ignition configuration for fixed-size sample grids. Larger and wider sample grids could be interpreted as analogous to broader fires because all windward cells were ignited. Larger grids have more possible fire travel routes and thus more routes offering faster spread. Some observations of wildland fire behavior are consistent with this interpretation. Rothermel (1991) observed that larger fires were less sensitive to obstacles and more likely to somewhere exhibit extreme behavior (independent of fire behavior or burning conditions). Large fires more rapidly find ways to cross streams, roads, rocks, etc., and are more likely to find fuel types conducive to fast spread (Rothermel 1991). Small or narrow fires (relative to the scale of heterogeneity) are more likely to be constrained by slower-burning fuel types or obstacles (or at least delayed for longer periods until a route is found through, over, or across the slow-burning type). The increase in expected spread rate could be dramatic for point-source ignitions that must grow beyond a size where they are sensitive to the scale of the heterogeneity.

Although this technique assumes that fires are larger than the fuel heterogeneity, the magnitudes, scales, and patterns of topographic and fuel variation have been little studied with respect to fire behavior. Kalabokidis and Omi (1992) reported heterogeneity of fuel depth and loading at scales of 20–60 m within forest and brush fuel types. Indirectly, studies of fire effects and forest structure suggest heterogeneity at scales important to fire behavior. Plots within the Yellowstone fires from 1988 showed variable forest structure and fire effects at scales of 10–100 m (Turner *et al.* 1989). Larger forest patch sizes have been found to occur with more severe fire regimes. In 'Large-scale fire disturbance in Pacific Northwest Ecosystems'. (Agee 1998; DeLong 1998). Very large fires on real landscapes, however, will likely expand into non-constant mixtures of burning conditions and exceed the assumptions of this analysis. For example, large fires often cross elevation and vegetation zones, each with different mixtures of fuel types and topography. The dependence on relative fire size also means that there is no absolute method for choosing a given sample grid size or shape for representing fire spread rates. The results of the FARSITE simulations suggested that $n \times 3$ sample grids were sufficient for all fuel types and fire sizes tested. The simulations produced fires that had forward spread distances 10^2 to 10^3 greater than the size of the individual fuel cells. Much larger and wider fires with greater numbers of distinct fuel types may be better represented by larger grids, but will require further study.

The curves of the expected spread rates $E[r_2]$ and $E[r_{2,j}]$ were not symmetric over the range of changing proportions of two fuel types. Curves of $E[r_{2,j}]$ with very low *SRR* (0.01 and 0.001), however, must be plotted on a logarithmic ordinate to see the asymmetrical changes in spread rate over several orders of magnitude. The asymmetry suggests that fire growth responds differently in mixtures of fast- and slow-burning fuel types when one or the other type is rare. When the slow-burning fuel type was rare, an increase in its fraction had a negligible effect on the expected spread rate because the fire could circumvent the isolated patches; the fire incurred a small delay by flanking compared with being forced to spread through the slow-burning patches. The reverse was true when faster-burning fuels were rare. Increasing the fraction of faster-burning fuels caused a relatively rapid increase in the expected spread rate because the fire always took the opportunity to move through them rather than around them.

Results of this analysis have real implications for spatial strategies of fuel treatments on landscapes. Most important is that random or arbitrary patterns of treatments are unlikely to have a significant effect on the overall growth rate or size of wildfires until large fractions of the landscape are treated. The sigmoid curve form found for two fuel types illustrates that more than 20–30% of the landscape must be converted from a fast spreading type to a fuel with slower spread rate before $E[r_2]$ is substantially reduced. Furthermore, the effectiveness of the treatment inside a random patch is largely irrelevant to the overall spread rate until large proportions of the landscape are treated. This contrasts with an explicit spatial strategy using overlapping 'brick' treatments (Finney 2001) that produces an immediate reduction in expected spread rate with small fractions of the landscape treated. It also allows a smaller area to be treated if the treated areas have slower spread rates. Another difference is that random landscapes are expected to permit larger fires to spread faster than small fires. This is not the case with the brick-type pattern (Finney 2001), which maintains the same expected spread rate regardless of fire size because the amount of flanking spread is strictly controlled. It is clear then, that random placement of fuel treatments would be inefficient in reducing overall spread rates and sizes of wildland fires.

Conclusions

The harmonic mean was found to be useful for calculating an expected spread rate for 2-dimensional random fuels. The accuracy of the calculation, however, depended on the dimensions of the sample grid used for calculating minimum travel time (i.e. spread rate) and the relative spread rate of the slowest fuel type. A 3×3 cell sample grid produced good results when the slowest relative spread rate was about 0.1.

A wider grid (3 × 7 cells) was required when the slowest relative spread rate was 0.01. This 2-dimensional approach could provide better estimates of average fire spread rate in spatial fuel mixtures than the 1-dimensional harmonic mean and the arithmetic average, but requires calculating the elliptical fire shape dimensions from wind and slope. Analysis of random fuel configurations also suggests that large fires should spread faster than small fires and that random placement of fuel treatment units would be inefficient for changing gross fire spread rates.

Acknowledgements

The author is grateful to Mark Schaaf for his early support of this work and to the two anonymous referees who provided numerous suggestions for improving the paper.

References

Agee JK (1998) The landscape ecology of western forest fire regimes. In 'Large-scale fire disturbance in Pacific Northwest Ecosystems'. *Northwest Science* **72**, 24–34 (special issue).

Alexander ME (1985) Estimating the length-to-breadth ratio of elliptical forest fire patterns. Proceedings of the 8th Conference on Fire and Forest Meteorology, pp. 287–304.

Anderson DG, Catchpole EA, DeMestre NJ, Parkes T (1982) Modeling the spread of grass fires. *Journal of the Australian Mathematical Society (Series B)* **23**, 451–466.

Anderson HE (1982) Aids to determining fuel models for estimating fire behavior. USDA Forest Service General Technical Report INT–122. 22 pp.

Anderson HE (1983) Predicting wind-driven wildland fire size and shape. USDA Forest Service, Research Paper INT-305.

Anderson K, Powell S, Etches M (1998) A modified suppression response decision support system for Wood Buffalo National Park. Proceedings of the 2nd Symposium on Fire and Forest Meteorology pp. 32–37.

Andrews PL (1986) BEHAVE: fire behavior prediction and fuel modeling system–BURN subsystem, Part 1. USDA Forest Service General Technical Report INT–194. 130 pp.

Brown JK (1981) Bulk densities of nonuniform surface fuels and their application to fire modeling. *Forest Science* **27**(4), 667–683.

Brown JK (1982) Fuel and fire behavior prediction in big sagebrush. USDA Forest Service Research Paper INT-290.

Catchpole EA, de Mestre NJ, Gill AM (1982) Intensity of fire at its perimeter. *Australian Forest Research* **12**, 47–54.

Catchpole EA, Hatton TJ, Catchpole WR (1989) Fire spread through nonhomogeneous fuel modeled as a Markov process. *Ecological Modelling* **48**, 101–112.

Catchpole WR, Catchpole EA, Butler BW, Rothermel RC, Morris GA, Latham DJ (1998) Rate of spread of free-burning fires in woody fuels in a wind tunnel. *Combustion Science and Technology* **131**, 1–37.

Cheng N, House L (1996) Minimum travel time calculation in 3-D graph theory. *Geophysics* **61**(6), 1895–1898.

DeLong SC (1998) Natural disturbance rates and patch size distribution of forests in northern British Columbia: implications for forest management. In 'Large-scale fire disturbance in Pacific Northwest Ecosystems'. *Northwest Science* **72**, 35–48 (special issue).

Finney MA (1998) FARSITE: Fire Area Simulator–Model development and evaluation. USDA Forest Service, Rocky Mountain Research Station Research Paper RMRS-RP-4. Ogden, UT. 47 pp.

Finney MA (2001) Design of regular landscape fuel treatment patterns for modifying fire growth and behavior. *Forest Science* **47**(2), 219–228.

Finney MA (2002) Fire growth using minimum travel time methods. *Canadian Journal of Forest Reseach* **32**(8), 1420–1424.

Forestry Canada Fire Danger Group (1992) Development and structure of the Canadian Forest Fire Behavior Prediction System. Information Report ST-X-3. (Canadian Forest Service: Ottawa)

Frandsen WH, Andrews PL (1979) Fire behavior in nonuniform fuels. USDA Forest Service, Intermountain Forest and Range Experiment Station Research Paper INT–232. Ogden, UT. 34 pp.

Fried JS, Gilless JK, Martin RE (1988) CFES—The California Fire Economics Simulator: A computerized system for wildland fire protection planning. USDA Forest Service, Pacific Southwest Research Station General Technical Report PSW–101. pp. 212–217. Albany CA.

Fujioka FM (1985) Estimating wildland fire rate of spread in a spatially non-uniform environment. *Forest Science* **31**(3), 21–29.

Kalabokidis KD, Omi PN (1992) Quadrat analysis of wildland fuel spatial variability. *International Journal of Wildland Fire* **2**(4), 145–152.

Martin RE (1988) Rate of spread calculation for two fuels. *Western Journal of Applied Forestry* **3**(2), 54–55.

Moser TJ (1991) Shortest path calculation of seismic rays: *Geophysics* **56**(1), 59–67.

Richards GD (1990) An elliptical growth model of forest fire fronts and its numerical solution. *International Journal of Numerical Methods in Engineering* **30**, 1163–1179.

Richards GD (1995) A general mathematical framework for modeling two-dimensional wildland fire spread. *International Journal of Wildland Fire* **5**(2), 63–72.

Richards GD (2000) The mathematical modeling and computer simulation of wildland fire perimeter growth over a 3-dimensional surface. *International Journal of Wildland Fire* **9**(3), 213–221.

Rothermel RC (1972) A mathematical model for predicting fire spread in wildland fuels. USDA Forest Service, Intermountain Forest and Range Experiment Station Research Paper INT–115. Ogden, UT. 40 pp.

Rothermel RC (1983) How to predict the spread and intensity of forest and range fires. USDA Forest Service, Intermountain Forest and Range Experiment Station General Technical Report INT–143. Ogden, UT. 161 pp.

Rothermel RC (1991) Predicting behavior of the 1988 Yellowstone Fires: Projections versus reality. *International Journal of Wildland Fire* **1**(1), 1–10.

Salazar LA (1985) Sensitivity of fire behavior simulations to fuel model variations. USDA Forest Service Research Paper PSW-178.

Schaaf M, Wiitala M, Carlton D, Snell K, Ottmar R (1998) Modeling the tradeoffs between prescribed fire and wildfire emissions in forest and rangeland ecosystems. In 'Proceedings of the Third International Conference on Forest Fire Research and 14th Confrerence on Fire and Forest Meteorology, Luso, Portugal, 16–20 November 1998'. pp. 1673–1685.

Taplin RH (1993) Sources of variation for fire spread rate in non-homogeneous fuel. *Ecological Modelling* **68**, 205–211.

Turner MG, Gardner RH, Dale VH, O'Neill RV (1989) Predicting the spread of disturbance across heterogeneous landscapes. *Oikos* **55**, 121–129.

USDA Forest Service (1987) National fire management analysis and planning handbook. Forest Service Handbook 5109.19. Washington, D.C.

Van Wagner CE (1969) A simple fire growth model. *Forestry Chronicle* **45**, 103–104.

Wiitala MR, Carlton DW (1994) Assessing long-term fire movement risk in wilderness fire management. Proceedings of the 12th conference on Fire and Forest Meteorology, 26–28 October, Jekyll Island, Georgia. (Society of American Foresters: Bethesda MD)